Analysis, Control, and Operational Optimization of a *Zymomonas mobilis* Reactor with Equilibrium Multiplicity

Jorge O. Trierweiler and Fabio C. Diehl

Group of Intensification, Modeling, Simulation, Control and Optimization of Processes – GIMSCOP
Department of Chemical Engineering, Federal University of Rio Grande do Sul – UFRGS
Rua Luiz Englert, s/n CEP: 90040-040 - Porto Alegre - RS - BRAZIL
E-MAIL: {jorge, fcdiehl}@enq.ufrgs.br

Abstract: For a successful application of any industrial *Z. mobilis* facility, it is necessary to have an efficient and simple control strategy. This paper analyzes the control and optimization problem of a continuous ZM bioreactor modeled by Jöbses et al. (1986). This system has steady state multiplicity in part of the operating range. The idea is to maintain the process close to the manifold border where is achievable the highest ethanol production. Based on a systematically analysis of the operational controllability using the nonlinear RPN indices it is identified that the process can be controlled using a linear controller. Finally the paper proposes a variable transformation that makes easy to maintain the bioreactor close to the optimum.

Keywords: nonlinear degree measurement, RPN methodology, bifurcation, bioreactor control, process optimization

1 INTRODUCTION

Zymomonas mobilis has attracted considerable interest over the past decades as a result of its unique metabolism and ability to rapidly and efficiently produce ethanol from simple sugars. However, despite its apparent advantages of higher yields and faster specific rates when compared to yeasts, no commercial scale fermentations currently exist which use *Z. mobilis* for the manufacture of fuel ethanol. In addition to ethanol depending on the substrate other fermentation products can occur, such as lactic acid, acetic acid, formic acid, acetone, and sorbitol. See (Rogers *et al.*, 2007), for a detailed review.

In the literature, *Zymomonas mobilis* has been proposed as a more promising microorganism than conventional yeast *Saccharomyces cerevisiae* for industrial production of ethanol (Rogers *et al.*, 2007). A major drawback of this microorganism is that it exhibits sustained oscillations (i.e., Hopf bifurcation) for low dilution rates (i.e., $D_f \leq 0.1\ h^{-1}$) when grown in continuous mode. This leads to decreased ethanol productivity and less efficient use of available substrate (Zhang and Henson, 2001). Various models have been proposed to describe the oscillatory dynamics of continuous *Zymomonas mobilis* cultures. Two of them are the Daugulis *et al.* (1997) and Jöbses *et al.* (1986) models. Even though the model predictions can be considered similar at low dilution rates, where the models have been fitted to the experimental data, they are quite different for higher dilution rates (Trierweiler and Diehl, 2009).

The Jöbses's model was fitted to experimental data with low dilution rate (i.e., $D_f \leq 0.1\ h^{-1}$) and middle inlet substrate concentration (i.e., $C_{S0} \cong 150\ kg/m^3$). Later, it was extrapolated outside of this operating region by Elnashaie *et al.* (2006), who have found a much more profitable operating region at higher dilution rates ($D_f \cong 2.0\ h^{-1}$) and inlet concentrations ($C_{S0} \cong 200\ kg/m^3$). Notwithstanding the Jöbses's model has not been validated at this region, our contribution will assume that this extrapolation is acceptable and we will propose a control strategy to maintain the system working at this more profitable operating region.

This paper is structured as follows: In section 2 the Jöbses's models is presented, section 3 it is analyzed the operational controllability which is used as basis for the proposed control strategy developed in section 4 and later validated by simulation. Final conclusions and remarks are then summarized in section 5.

2 MODEL DESCRIPTION AND OPERATING POINT DEFINITIONS

Since the Jöbses's model can predict a branch with higher ethanol production, which has been experimentally confirmed (at least for low dilution rates) by Elnashaie *et al.* (2006), we decide to analyze the control problem of a continuous bioreactor with the Jöbses *et al.* (1986) kinetic model, which is shortly described in the next subsection.

2.1 *Model Description*

The Jöbses's model consists of the following 4 differential equations:

$$\frac{dC_S}{dt} = -\frac{\mu_{max}.C_S.C_E}{Y_{SX}.(K_S+C_S)} - m_S.C_X + D_f.(C_{S0} - C_S)$$

$$\frac{dC_X}{dt} = \frac{\mu_{max}.C_S.C_E}{(K_S+C_S)} + D_f.(C_{X0} - C_X) \quad (1)$$

$$\frac{dC_E}{dt} = \frac{K_E.(C_P-c_1)(C_P-c_2).C_S.C_E}{(K_S+C_S)} + D_f.(C_{E0} - C_E)$$

$$\frac{dC_P}{dt} = \frac{\mu_{max}.C_S.C_E}{Y_{PX}.(K_S+C_S)} + m_P.C_X + D_f.(C_{P0} - C_P)$$

where C_S is the substrate (glucose) concentration, C_X is the biomass (*Z. mobilis*), C_P is the product (ethanol) concentration, and C_E is an auxiliary variable used to lag the effect of the ethanol concentration in the kinetic model. The insertion of the $K_E.(C_P - c_1)(C_P - c_2)$ parcel together with C_E makes possible the model to depict the oscillatory behavior of the Hopf bifurcation. In the model, dilution rate D_f is the inversion of the residence time and is defined as the relation between the inlet flow rate and the bioreactor volume. The model parameters are summarized in Table 1.

Table 1: Model parameters

Parameters	Values	Parameters	Values
$K_E\ \left[\frac{m^6}{kg^2.h}\right]$	0.00383	$m_S\ \left[\frac{kg}{kg.h}\right]$	2.160
$c_1\ \left[\frac{kg}{m^3}\right]$	59.2085	$m_P\ \left[\frac{kg}{kg.h}\right]$	1.100
$c_2\ \left[\frac{kg}{m^3}\right]$	70.5565	$(Y_{SX}, Y_{PX})\ \left[\frac{kg}{kg}\right]$	(0.02445, 0.05263)
$K_S\ \left[\frac{kg}{m^3}\right]$	0.500	$\mu_{max}\ \left[\frac{1}{h}\right]$	1.0

Fig. 1 shows the steady-state solutions for ethanol concentration (C_P) in function of dilution rate (D_f) and inlet substrate concentration (C_{S0}).

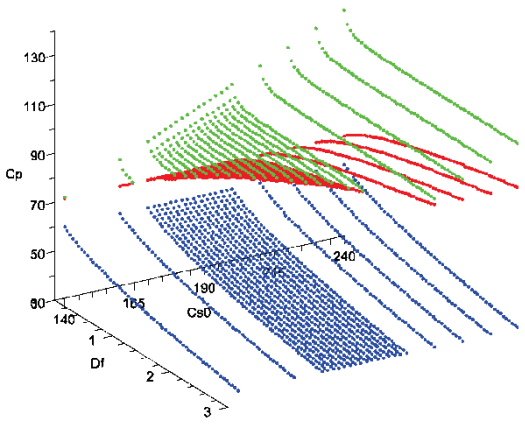

Fig. 1: Steady-state ethanol concentration (C_P) as a function of Dilution rate (Df) and inlet substrate concentration (C_{S0}).

2.2 *Operating points*

The optimal condition for the bioreactor is achieved with a high ethanol production. For the Jöbses's model, it can be shown that the main decision operating criterion for the best operating point is the ethanol production (EP), which is given by the multiplication of the dilution rate (D_f) and the ethanol concentration (C_P), i.e.,

$$EP = D_f.C_P. \quad (2)$$

Fig. 2 is produced for the iso-inlet substrate concentrations C_{S0} of 180, 200, and 220 kg/m^3 that were already shown in Fig. 1. Note that the dashed and dashdot lines are the same for all three operating conditions, therefore only one line for each branch is shown in Fig. 2.

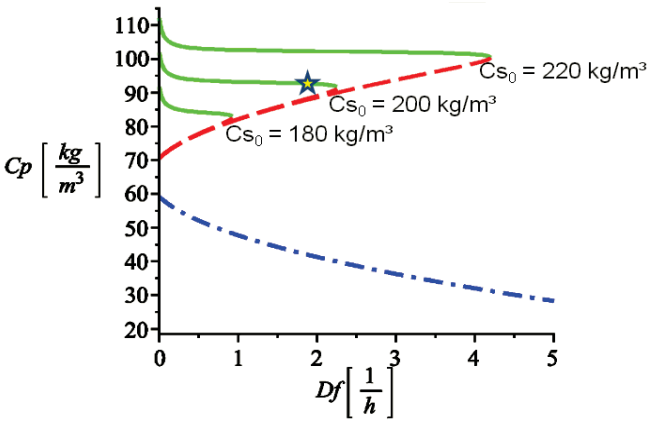

Fig. 2: Steady-state ethanol concentration (C_P) for three inlet substrate concentrations (C_{S0}).

Considering the curves generated for $C_{S0} = 200\ kg/m^3$ in Fig. 2, we can see that in the range of $0 < D_f < 2.25\ h^{-1}$ the system has three possible steady-state solutions. Two of them are stables (solid and dashdot lines) and one unstable (i.e., the middle branch illustrated by dashed line). The best operating point is located in the above curve close to the saddle point formatted by the intersection of the stable and unstable branches. The star in the above branch depicts a typical optimal operating point. From a control point of view the main difficult is to maintain the system working in this point avoiding a migration to the bellow operating point – the dash-dot line in Fig. 2. This migration can occur if the dilution rate is above the corresponding to the bifurcation saddle point or by a reduction to the inlet substrate concentration. Fig. 3 shows the case where the dilution rate is increased from 2 h^{-1} to 2.5 h^{-1} and then at 10 h again reduced to 2 h^{-1}. To bring the system to the more profitable operating point it is necessary to apply a pulse in the inlet ethanol concentration (C_{P0}) as shown at 15 h.

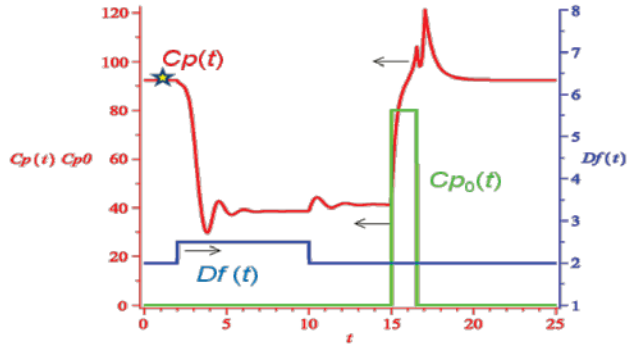

Fig. 3: Dynamic simulation to show how it is easy to move the operating point from the high to the low production branch.

2.3 Operating regions

The manifold that separate the region where occurs multiplicity in the ethanol concentration is defined by the saddle bifurcation points and is shown in Fig. 4. This manifold limits the operating region with possible high ethanol concentration (region A) from the region where only a low ethanol concentration is achievable (region B), where the operating conditions goes outside de operating region A, the ethanol concentration will fall down as it was depicted in Fig. 3.

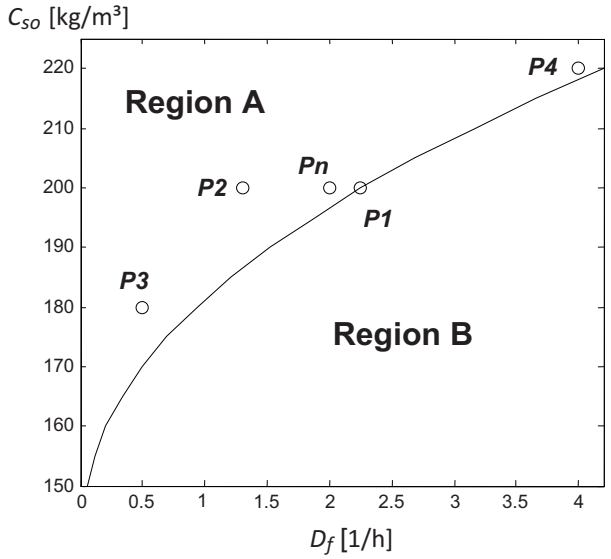

Fig. 4: Manifold of saddle points defining the operating region A (where exists multiplicity) and operating region B (where exits one solution only).

To characterize the differences between the high and low ethanol concentration branches, the system was linearized in five different operating points defined in Table 2 and placed in Fig. 4, where P_n is considered as the nominal/optimal operating point. The other four can occurs during a normal operation in the region A. Of course, P_4 has higher *EP* than P_n, but since the Jöbses model cannot describe higher C_{S0} correctly, we will just assume that P_n is the best operating point, but the same analysis could be performed considering P_4 as nominal model.

Table 2: Definition of Operating Region

	D_f $[h^{-1}]$	$C_{S0}\left[\frac{kg}{m^3}\right]$	OP1- high C_P $(C_P, C_S)_{SS}$*	OP2 - low C_P $(C_P, C_S)_{SS}$*
P_n	2.0	200	(92.57, 1.23)	(41.29, 111.34)
P_1	2.25	200	(91.83, 2.75)	(39.94,114,22)
P_2	1.3	200	(93.07, 0.40)	(45.56, 102.29)
P_3	0.5	180	(84.24, 0.31)	(52.09,68.90)
P_4	4.0	220	(101.38, 2.04)	(32.02, 151.16)

*$(C_P, C_S)_{SS}$ means steady-state values for ethanol and substrate concentration for a given D_f and C_{S0}.

Figures 5 and 6 respectively show the step response of the dynamic linearized models for high and low ethanol concentration branches. Essentially the high ethanol branch has an over-damped behavior, whereas for the low branch the system is under-damped.

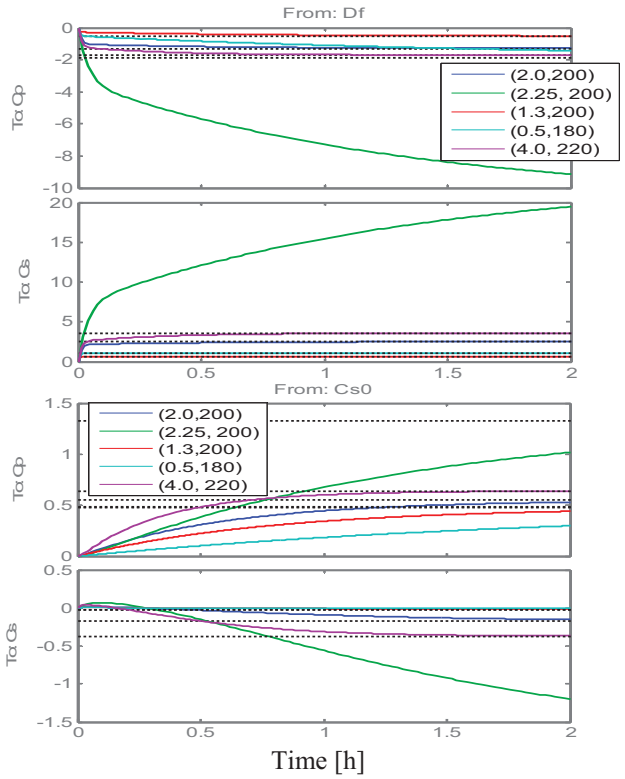

Fig. 5: Step response of the linearized models at the operating points defined in Table 2 corresponding to the high ethanol concentration branch for C_P and C_S outputs.

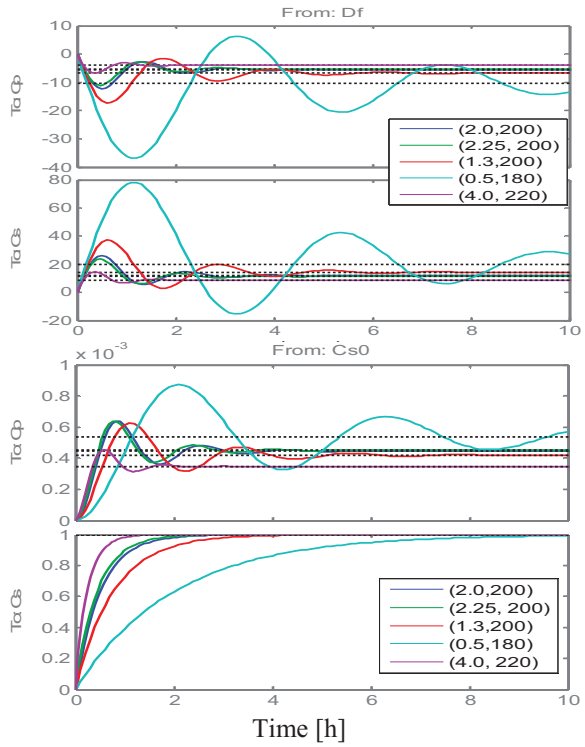

Fig. 6: Step response of the linearized models at the operating points defined in Table 2 corresponding to the low ethanol concentration branch for C_P and C_S outputs.

3 OPERATIONAL CONTROLLABILITY ANALYSIS

3.1 Manipulated and controlled variables

Ethanol and substrate concentrations are two natural controlled variables of the system and can be in principle measured on-line using 2D-fluorescence spectroscopy (Hantelmann *et al.*, 2006). As candidates for manipulated variables, we have the dilution rate (D_f), inlet substrate concentration (C_{S0}), and inlet ethanol concentration (C_{P0}). In principle, C_{P0} should be used only in critical situations, just to bring the system back to the higher production branch (as shown in Fig. 3). Therefore we will not consider it in our operational controllability analyses, where only the input-output pairs $(D_f, C_{S0}) \rightarrow (C_P, C_S)$ is further considered.

3.2 Nominal Operational Controllability

The determinant and the elements λ_{11} and λ_{12} of the RGA – relative gain array (Skogestad and Postlethwaite, 2005) – are calculated using the steady state gain matrix for each one of the linearized models defined in Table 2. These results are summarized in Table 3, where we can see that the determinant (Det) does not change its sign when the system goes from the operating region 1 (OR1) with high ethanol concentration to OR2 with low ethanol concentration. Nevertheless the recommended pairing using steady state RGA changes from OR1 to OR2. Usually, when the pairing recommendation is changed it is normally associated with a change in the determinant sign, what it does not happens for this system. When the determinant changes its sign it is equivalent to the change in the multivariable gain, what is quite critical for the success of any control strategy. The reason for this unusual behavior is related to the gain sign change of channel $C_{S0} \rightarrow C_S$ ($i.e., K_{22}$) as it can been seem by the gain matrix for the nominal operating point P_N for the high and low ethanol concentration branches, which are given by:

$$K_{PN\_high} = \begin{bmatrix} -1.30 & 0.55 \\ 2.55 & -0.18 \end{bmatrix} \quad (3)$$

$$K_{PN\_low} = \begin{bmatrix} -5.55 & 0.0004 \\ 11.82 & 0.999 \end{bmatrix} \quad (4)$$

Similar behavior occurs for all other OPs.

Table 3: Determinant and Steady State RGA

	Det OR1	Det OR2	RGA – OR1 $(\lambda_{11}, \lambda_{12})$*	RGA – OR2 $(\lambda_{11}, \lambda_{12})$*
P_n	-1.16	-5.55	(-0.20, 1.20)	(0.99, 0.01)
P_1	-10.58	-5.25	(-1.89, 2.89)	(0.99, 0.01)
P_2	-0.26	-6.78	(-0.05, 1.05)	(0.99, 0.01)
P_3	-0.48	-10.26	(-0.11, 1.11)	(0.99, 0.01)
P_4	-1.66	-3.98	(-0.38, 1.38)	(0.999, 0.001)

$(\lambda_{11}, \lambda_{12})$* it was calculated considering the pairing $D_f \rightarrow C_P$ and $C_{S0} \rightarrow C_S$.

3.3 RPN and rRPN Analysis

The Robust Performance Number (RPN) was introduced in (Trierweiler, 1997) and (Trierweiler and Engell, 1997) as a measure to characterize the operational controllability of a system. The RPN indicates how potentially difficult it is for a given system to achieve the desired performance robustly. The RPN is influenced by three terms: the desired closed loop performance, nonminimum phase behavior (i.e., RHP pole, zero, and pure time delays), and its degree of directionality.

The RPN is a measure of how potentially difficult it is for a given system to achieve the desired performance robustly. The easiest way to design a controller is to use the inverse of the process model. An inverse-based controller will have potentially good performance robustness only when the RPN is small. As inverse-based controllers are simple and effective, it can be concluded that a good control structure selection is one with a small (< 5) RPN (Trierweiler and Engell, 1997).

Table 4: RPN Analysis for the *high* ethanol concentration branch

	$t_R = 1.0\ h$		$t_R = 0.50\ h$		$t_R = 0.25\ h$	
	RPN	$rRPN$	RPN	$rRPN$	RPN	$rRPN$
P_n	1.66	0.088	1.61	0.085	1.58	0.086
P_1	2.27	0.152	1.90	0.1201	1.78	0.097
P_2	1.52	0.069	1.53	0.074	1.51	0.0790
P_3	1.50	0.068	1.53	0.0725	1.52	0.0781
P_4	1.91	0.124	1.80	0.110	1.69	0.101

Table 4 shows the RPN calculated by three different desired performance specified by the rise times $t_R = 1, 0.5,$ and $0.25\ h$ and 10% overshoot for both outputs, what makes the system 2, 4, and 8 times faster than open loop response for the high ethanol concentration branch and all operating points. The results shown in Table 4 allow us to conclude that considering each operating point independently they will be easily controllable. It is important to mention that the RPN does not give a clear idea of the control difficulties for that it is necessary to analyze the *relative* RPN ($rRPN$), which has been introduced by Trierweiler (2002) (see also (Trierweiler and Farina, 2002) for an additional discussion).

The $rRPN$ is the relative distance between the RPN curve and the minimum RPN curve and it is quantified by the areas under the curves. Values less than 1 and close to zero means that the desired performance is easily achievable. Again, since we are considering only the two stable branches, no nonminimum phase component occurs in the analyzed operating points. In this case, typically faster performance will usually reduce the $rRPN$. Table 4 depicts that it is possible to design a controller that achieves the desired performance for each one of the analyzed operating points. Similar analyses (not shown here) performed for the low ethanol concentration branch produce similar conclusions with a RPN and $rRPN$ in the order of 1.5 and 0.004, respect.

The local operational controllability analyses clearly conclude that for each one of the considered models it is possible and easy to design a controller with the desired performance. Although each point is easily controllable,

nothing can be said about all operating points together. Is there possible to design a controller that will produce a good performance for all operating points? Moreover, if a controller designed for OR1 will work in OR2? Based on the steps responses of the linearized models shown in Figures 5 and 6, it seems the responses are quite different, especially if we compare the under-damped behavior shown by OR2 and the over-damped of the OR1. In the next subsection, we answer these questions through the *nonlinear RPN* analysis.

3.4 Nonlinear degree – nRPN Analysis

In (Farenzena and Trierweiler, 2004) three novel indices were introduced to measure system's nonlinearity. These nonlinear measurements are derived from the Robust Performance Number (RPN) concept. The total system's nonlinearity can be measured by the *nonlinear RPN* ($nRPN$), while the purely static nonlinearity is captured by *nonlinear static RPN* ($nRPN_{STAT}$) and the dynamic component by the *nonlinear dynamic RPN* ($nRPN_{DYN}$). These indices do not require a nonlinear model, being enough a set of linear models. Therefore, they can easily be applied to quantify the nonlinearities of industrial plants and used to answer several practical important questions such as: how nonlinear is the system? Is it necessary to apply a nonlinear controller? What kind of nonlinear controller is required?

In the definition of the nonlinear RPN indices was introduced the logarithm function to make easier their interpretation. Values smaller than 1 indicate that the performance difference between nonlinear and linear controllers is not significant, so that a linear controller is recommended. Indices greater than 2 clearly indicate that a nonlinear controller is necessary. Between 1 and 2 is a transition zone, where in many times a robust controller can stabilize all possible plants, but the performance loss can be significant if the values are close to 2. This analysis is made for all three indices. For instance, if $nRPN$ and $nRPN_{STAT}$ are high and $nRPN_{DYN}$ is small, it indicates that the nonlinearity is essentially static and can be compensated by gain scheduling controller. If the all values are big (greater or close to 2), then a nonlinear model predictive controller is recommended.

Table 5: $nRPN$, $nRPN_{STAT}$, and $nRPN_{DYN}$. Analyses

	$t_R = 1.0\ h$			$t_R = 0.50\ h$		
	nRPN	*STAT.*	*DYN.*	*nRPN*	*STAT.*	*DYN.*
H	0.86	0.58	-0.052	0.79	0.58	-0.21
L	0.31	-0.28	0.455	0.27	-0.28	0.40
T	1.68	0.88	0.74	1.50	0.88	0.51
	$t_R = 0.25\ h$			$t_R = 0.10\ h$		
	nRPN	*STAT.*	*DYN.*	*nRPN*	*STAT.*	*DYN.*
H	0.74	0.58	-0.35	0.69	0.58	-0.54
L	0.27	-0.28	0.39	0.29	-0.28	0.42
T	1.32	0.88	0.24	1.12	0.88	-0.12

→ Stat. and Dyn. mean $nRPN_{STAT}$ and $nRPN_{DYN}$, respect. *H*: polytope model for the high C_P branch, *L*: polytope model for the low C_P branch, and $T = H \cup L$.

To quantify the nonlinearity using the *nonlinear RPN* it is necessary to construct a set of linearized models, called as polytope model. The operating points defined in Table 2 have been used to define the polytopes. Three polytope sets have being formed: *H* formed with the 5 linearized models at the *high* ethanol concentration branch; *L* formed from the linearized models corresponding to the *low* C_P branch; and *T* formed by the union of all 10 models.

Table 5 summarizes the results of the $nRPN$ analysis, which indicates that in general the polytope *H* is more nonlinear than the polytope *L* and the nonlinearity found in *H* is essentially static, whereas for *L* the nonlinearity is of the dynamic type. Of course, the combination of both polytopes (*T*) exhibits the highest nonlinearity, which has similar dynamic and static components for low performance, but for the highest desired performance (i. e., $t_R = 0.10$) it becomes essentially static. Moreover, for this performance it is expected that a linear controller will be able to control the system in both operating regions. To verify this prediction, we have design a multivariable PI controller, given by:

$$PI(s) = \begin{bmatrix} -0.161 \times \left(1 + \frac{1}{0.1128s}\right) & 1.6981 \times \left(1 + \frac{1}{0.0063s}\right) \\ 12.287 \times \left(1 + \frac{1}{0.6288s}\right) & 6.4204 \times \left(1 + \frac{1}{0.3606s}\right) \end{bmatrix} \quad (5)$$

This quite simple controller can control all 10 linearized models with a good performance as it is shown in Fig. 7, where it has been simulated a setpoint change in C_P of one unit at 1 h and a simultaneous load disturbance of $\Delta D_f = 0.2\ h^{-1}$ and $\Delta C_{S0} = 1\ kg/m^3$ at 6 h.

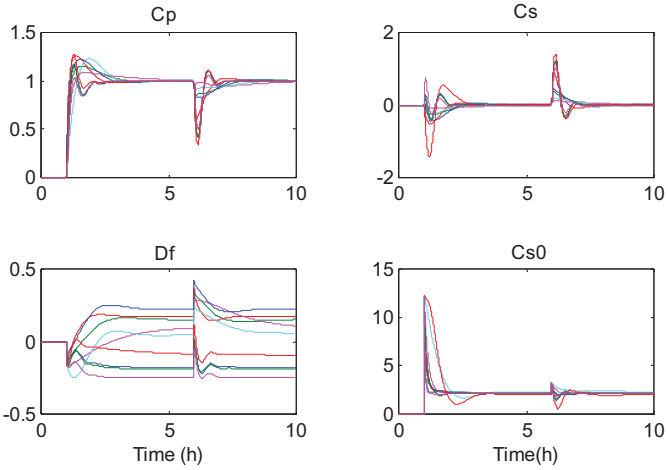

Fig. 7: Closed loop simulation with a multivariable *PI* controller for all 10 linearized models

4 CONTROL STRATEGY

Note that the predictions made by nonlinear RPN indices were confirmed by the closed loop simulation using the linearized models. Similar results are obtained using the fully nonlinear model (Trierweiler and Diehl, 2009). In this section, it is shown the basic ideas of the recommended control strategy.

4.1 General control strategy

It is recommended to use an Extended Kalman Filter (EKF) technique to filter the measurements from the 2D-fluorescence spectroscopy. The EKF is important also to estimate the biomass concentration and to take the input and model uncertainties into account. A multivariable controller should be used with the pairing $(D_f, C_{S0}) \rightarrow (C_P, C_S)$ and the inlet ethanol concentration (C_{P0}) should be only used in exceptional cases to bring the system back to the high ethanol concentration branch as shown in Fig. 3.

4.2 Solving the constraint problem

A single linear controller can be used to control the bioreactor in all operating conditions. The only special problem is to constraint the range of the manipulated variables, which should be limited by the saddle point manifold. This can be easily guaranteed by a single variable transformation as shown in Fig. 8. Instead to use directly the physical variables $(\Delta C_{S0},\ \Delta D_f)$ the controller calculate the control actions for $(\Delta y,\ \Delta x)$ using the simple restriction $\Delta y > 0$. The conversion to $(\Delta C_{S0},\ \Delta D_f)$ is performed by the multiplication with the rotation matrix R, given by:

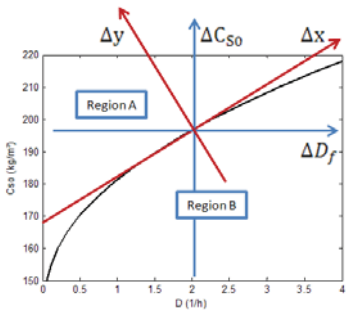

$$R = \begin{bmatrix} \cos(\theta) & -\sin(\theta) \\ \sin(\theta) & \cos(\theta) \end{bmatrix}$$

where θ is the rotation angle.

Fig. 8: Simple variable transformation for guarantee the feasible region A

Note that the optimal operating point is close to $\Delta y = 0$. This idea is explored in (Trierweiler and Diehl, 2009) to maintain the system always close to the optimal economic conditions.

5 CONCLUSIONS

The paper has introduced several contributions, which are summarized as follows:

***Zymomonas mobilis* control problem** – as far as we know, this contribution is the first paper that discusses the control problem of a continuous bioreactor with *Z. mobilis*.

Control strategy – a simple and efficient control strategy has been proposed based on the control of (C_P, C_S) using the manipulated variables $(\Delta C_{S0},\ \Delta D_f)$. Since the branch where the high C_P occurs is restricted, it was proposed to use a variable transformation as shown in Fig. 8. This transformation makes simple to consider the restriction range and open a simple strategy for assuring the optimal economic conditions, which occurs at $\Delta y \approx 0.5$.

RGA pairing with negative diagonal elements – the *Z. mobilis* bioreactor with the Jöbses's model it is a interesting example to illustrate that the common pairing rule where the positive diagonal elements are recommended it is not always the best global pairing. For this system the best pairing changes when the system moves from the high to the low C_P branch. It is interesting that the paring change occurs without alteration in the sign of the gain matrix determinant.

The RPN analysis is reliable – the RPN analysis, especially using the nonlinear RPN indices made possible very easily to check and quantify the nonlinearity degree and based on these analyses prescribe the appropriated controller. It was shown that if a fast controller is designed a simple linear controller can be used. To confirm this prediction a simple multivariable PI controller has been tuned and simulated.

Procedure for analysis a bioprocess optimization and control problem – finally the paper illustrate the typical steps necessary to develop a control and optimization strategy for a bioprocess system. Before designing a controller, it is necessary to systematically analyze the system as have been done in the paper.

Jöbses's Model – we have assumed that the model could predict the system behavior at high dilution rate and inlet substrate concentration. Of course, this extrapolation is totally questionable considering a real application.

Acknowledgements: The authors are very grateful for the grants from CAPES / BRAZIL. The first author also thanks Prof. Dr. W. Marquardt for receiving him for his sabbatical at RWTH Aachen, where this work has been written.

REFERENCES

Daugulis, A. J., Mclellan, P. J. and Li, J. (1997) Experimental investigation and modeling of oscillatory behavior in the continuous culture of *Zymomonas mobilis*. *Biotechnology and Bioengineering,* 56**,** 99-105.

Elnashaie, S. S. E. H., Chen, Z., Garhyan, P., Prasad, P. and Mahecha-Botero, A. (2006) Practical Implications of Bifurcation and Chaos in Chemical and Biological Reaction Engineering. *International Journal of Chemical Reactor Engineering 4*

Farenzena, M. and Trierweiler, J. O. (2004) System Nonlinearity Measurement Based on the RPN Concept. *DYCOPS - 7TH IFAC Symp. on Dynamics and Control of Process Systems***,** 181-191.

Hantelmann, K., Kollecker, M., Hüll, D., Hitzmann, B. and Scheper, T. (2006) Two-dimensional fluorescence spectroscopy: A novel approach for controlling fed-batch cultivations. *Journal of Biotechnology,* 121**,** 410-417.

Jöbses, I. M. L., Egberts, G. T. C., Luyben, K. C. A. M. and Roels, J. A. (1986) Fermentation kinetics of *Zymomonas mobilis* at high ethanol concentrations: Oscillations in continuous cultures. *Biotechnology and Bioengineering,* 28**,** 868-877.

Rogers, P., Jeon, Y., Lee, K. and Lawford, H. (2007) Zymomonas mobilis for Fuel Ethanol and Higher Value Products. *Biofuels.* Springer Berlin / Heidelberg.

Skogestad, S. and Postlethwaite, I. (2005) *Multivariable feedback control : analysis and design,* Chichester, England ; Hoboken, NJ, John Wiley.

Trierweiler, J. O. (1997) A Systematic Approach to Control Structure Design. Dortmund, University of Dortmund.

Trierweiler, J. O. (2002) Application of the RPN Methodology for Quantification of the Operability of the Quadruple-Tank Process. *Brazilian Journal of Chemical Engineering,* 19**,** 195-206.

Trierweiler, J. O. and Diehl, F. C. (2009) Control Strategy for a *Zymomonas mobilis* Bioreactor used in the Ethanol Production. *Submitted to PSE 2009*

Trierweiler, J. O. and Engell, S. (1997) The Robust Performance Number: A New Tool for Control Structure Design. *Computer Chemical Engineering* 21**,** 237-243.

Trierweiler, J. O. and Farina, L. A. (2002) The RPN Methodology Applied to Quantify Process Operability and Controller Design. *Proc.15th IFAC World Congress, Barcelona***,** CDROM, paper 2663.

Zhang, Y. and Henson, M. A. (2001) Bifurcation Analysis of Continuous Biochemical Reactor Models. *Biotechnology Progress,* 17**,** 647-660.